Cancer Research

CCL2 Mediates Cross-talk between Cancer Cells and Stromal Fibroblasts That Regulates Breast Cancer Stem Cells

Akihiro Tsuyada[1,7,8], Amy Chow[1], Jun Wu[2], George Somlo[3], Peiguo Chu[4], Sofia Loera[4], Thehang Luu[3], Arthur Xuejun Li[5], Xiwei Wu[6], Wei Ye[5], Shiuan Chen[1], Weiying Zhou[1], Yang Yu[1,9], Yuan-Zhong Wang[1], Xiubao Ren[9], Hui Li[9], Peggy Scherle[10], Yukio Kuroki[7], and Shizhen Emily Wang[1]

Abstract

Cancer stem cells (CSC) play critical roles in cancer initiation, progression, and therapeutic refractoriness. Although many studies have focused on the genes and pathways involved in stemness, characterization of the factors in the tumor microenvironment that regulate CSCs is lacking. In this study, we investigated the effects of stromal fibroblasts on breast cancer stem cells. We found that compared with normal fibroblasts, primary cancer-associated fibroblasts (CAF) and fibroblasts activated by cocultured breast cancer cells produce higher levels of chemokine (C-C motif) ligand 2 (CCL2), which stimulates the stem cell–specific, sphere-forming phenotype in breast cancer cells and CSC self-renewal. Increased CCL2 expression in activated fibroblasts required STAT3 activation by diverse breast cancer–secreted cytokines, and in turn, induced NOTCH1 expression and the CSC features in breast cancer cells, constituting a cancer-stroma-cancer signaling circuit. In a xenograft model of paired fibroblasts and breast cancer tumor cells, loss of CCL2 significantly inhibited tumorigenesis and NOTCH1 expression. In addition, upregulation of both NOTCH1 and CCL2 was associated with poor differentiation in primary breast cancers, further supporting the observation that NOTCH1 is regulated by CCL2. Our findings therefore suggest that CCL2 represents a potential therapeutic target that can block the cancer–host communication that prompts CSC-mediated disease progression. *Cancer Res; 72(11); 2768–79. ©2012 AACR.*

Introduction

Recent studies indicate that a subset of cancer cells possessing stem cell properties, referred to as cancer-initiating or cancer stem cells (CSC), play crucial roles in tumor initiation, progression, and therapeutic refractoriness (1, 2). Similar to embryonic and somatic stem cells, the self-renewal and differentiation of CSCs are simultaneously regulated by intrinsic (cancer cell–endowed) and extrinsic (microenvironmental) factors. Despite the increasing number of studies on genes and pathways involved in cancer stemness, factors in the tumor microenvironment that regulate CSCs, and how cancer cells, in turn, modify the niche by influencing their neighboring cells remain largely uncharacterized. In this study, we focus on the regulation of CSCs by stromal fibroblasts, an important cellular component of the tumor-hosting niche in many human cancers, especially breast cancer. Fibroblasts release a variety of growth factors, chemokines, and components of the extracellular matrix into the microenvironment and influence the differentiation and homeostasis of adjacent epithelia (3). Reconstitution of human-specific mammary glands in cleared mouse mammary fat pads using stem cell–enriched human mammary epithelial cell organoids requires coinjection of human mammary fibroblasts (4), suggesting a critical role for fibroblasts in regulating stem cell functions. Fibroblasts interplay with cancer cells at all stages of cancer progression through complex paracrine mechanisms. Cancer-associated fibroblasts (CAF) can promote cancer progression by modulating multiple components in the cancer niche to build a permissive and supportive microenvironment for tumor growth and invasion.

In the current study, we observed a robust induction of the stem cell–like mammosphere-forming phenotype in breast cancer cells cocultured with CAFs. The CSC-stimulating effect was attributed to the increased secretion of CCL2 (monocyte chemotactic protein-1; MCP-1) by CAFs when compared with normal cell–associated fibroblasts (NAF). CCL2 signals through the G-protein–coupled receptor chemokine (C-C motif) receptors CCR2 and CCR4, and is a potent chemoattractant for monocytes and other immune cells to areas of inflammation (5). Both monocytic and nonmonocytic cells, such as fibroblasts and endothelial cells, secrete CCL2 in response to cytokine stimulation (6, 7). Cancer cells also

Authors' Affiliations: Divisions of [1]Tumor Cell Biology and [2]Comparative Medicine, Departments of [3]Medical Oncology, [4]Pathology, and [5]Information Science, [6]Bioinformatics Core Facility, City of Hope Beckman Research Institute and Medical Center, Duarte, California; [7]Department of Molecular Biology, [8]Graduate School of Medicine, Sapporo Medical University, Sapporo, Japan; [9]Department of Immunology & Biotherapy, Tianjin Cancer Hospital, Tianjin, China; and [10]Incyte Corporation, Wilmington, Delaware

Note: Supplementary data for this article are available at Cancer Research Online (http://cancerres.aacrjournals.org/).

Corresponding Author: Shizhen Emily Wang, Division of Tumor Cell Biology, Beckman Research Institute of City of Hope, 1500 E Duarte Road, KCRB Room 2007, Duarte, CA 91010. Phone: 626-256-4673, ext. 63118; Fax: 626-301-8972; E-mail: ewang@coh.org

doi: 10.1158/0008-5472.CAN-11-3567

frequently overexpress CCL2 to modify their local environment. Here, we further found that CCL2 induced the self-renewal of CSCs by inducing NOTCH1 expression at both RNA and protein levels. NOTCH signaling has been recognized as a key regulator in normal and malignant stem cells from various tissues, including the breast (8, 9). Upon ligand binding, NOTCH receptors are activated by sequential cleavages involving members of the ADAM (a disintegrin and metalloprotease domain) protease family (α-secretases) and γ-secretase. These cleavage events result in translocation of the NOTCH intracellular domain (NICD) to the nucleus, where it acts on downstream targets (10). Our identification of NOTCH-mediated activation by tumor environmental factor CCL2 therefore presents a unique mode of niche-conferred regulation of CSCs. These findings further emphasize the importance of simultaneously targeting cancer cells and events within the tumor microenvironment, such as production of CCL2 by stromal cells, in future anticancer therapies that also incorporate the latest stem cell research.

Materials and Methods

Tissue sources and cell purification

Human breast cancer tissues were obtained from consented patients at City of Hope Medical Center (Duarte, CA) under approved Institutional Review Board protocols. Tissues were mechanically and enzymatically dissociated, and epithelial tumor cells and fibroblasts (CAF) were isolated as previously described (11). Briefly, breast cancer tissue was mechanically minced into small pieces, placed in digestion solution containing collagenase III (Worthington Biochemical Corporation) and DNase I (AppliChem), and incubated at 37°C for 2 to 3 hours with occasional pipetting. The cells were separated by differential centrifugation at 90 × *g* for 2 minutes. The epithelial (tumor) cells in the pellet were cultured in Iscove's Modified Dulbecco's Media (Invitrogen) containing 0.7 mmol/L L-glutamine (Mediatech/Cellgro), 5 μg/mL insulin (Lonza), 5 μg/mL transferrin (Lonza), 5 ng/mL selenium (Lonza), and 20% FBS (PAA Laboratories). The supernatant containing fibroblasts were centrifuged at 800 × *g* for 10 minutes, resuspended and cultured in Dulbecco's Modified Eagle's Medium (Mediatech/Cellgro) containing 10% FBS on a nontreated dish. Purity of primary tumor cells and CAFs were confirmed by expression of epithelial-specific antigen (ESA) and vimentin, respectively, in flow cytometric and immunofluorescence assays (Supplementary Fig. S1). CAF265922 (primary CAFs) and XP265922 (primary tumor cells) were isolated from a primary triple-negative breast cancer that was resistant to the chemotherapy regimen containing cisplatin, 5-fluorouracil, and docetaxel. CAF3 were isolated from a primary HER2-positive breast cancer for which the primary tumor cells were not available. Normal human mammary fibroblasts (NAF2) were purchased from ScienCell. For immunohistochemistry in primary breast tumors, pretreatment core biopsies or surgical specimens were obtained from patients with HER2-positive (31 cases) or triple-negative ($ER^-/PR^-/HER2^-$; 20 cases) breast cancer. Specimens were collected and processed for formalin fixation and paraffin embedding in a time frame that would preserve the integrity of protein epitopes.

Cell lines, plasmids, and viruses

Human breast cancer cell lines BT474, MDA-MB-361 (MDA361), and MCF7, and the noncancerous mammary epithelial cell line MCF10A were obtained from American Type Culture Collection and cultured in the recommended media in a humidified 5% CO_2 incubator at 37°C. Recombinant human CCL2 was purchased from R&D Systems. The STAT3 inhibitor Stattic, p38 mitogen—activated protein kinase (MAPK) inhibitor SB202190, and γ-secretase inhibitor (GSI) DAPT were purchased from Sigma-Aldrich. The α-secretase inhibitor INCB3619 was provided by Incyte Corporation. For conditional knockdown of CCL2, the short hairpin RNA (shRNA) targeting the CCL2 mRNA (TRCN0000006283) was constructed into the pTIG (pHIV7-TetR-IRES-GFP) lentiviral vector (ref. 12; kindly provided by Dr. Rossi) downstream of a doxycycline-inducible U6 promoter, as described elsewhere (13). GFP-labeled CAF265922 were generated using pBABE-GFP retroviral vector. Production of viruses, as well as infection and selection of CAFs were carried out as previously described (13).

Mammosphere formation assay

Please see Supplementary Materials for procedures.

RNA extraction, reverse transcription, and quantitative real-time PCR

Please see Supplementary Materials for procedures.

Cytokine antibody array and Western blot analyses

Please see Supplementary Materials for procedures.

Cell transfection, reporter assays, and RNAi studies

Please see Supplementary Materials for procedures.

Flow cytometry and cell sorting

Single-cell suspensions prepared from tumors or cell culture were stained with allophycocyanin (APC)-conjugated human ESA antibody (catalog #347200; BD Biosciences) or analyzed by ALDEFLUOR assay kit (catalog #01700; Stemcell Technologies) following the manufacturer's protocol. Flow cytometric assays were conducted using a CyAn ADP cytometer (Dako) and analyzed with FlowJo software (TreeStar). Electronic cell sorting based on intensity of GFP, APC, PKH67, or ALDEFLUOR was done on a FACSAriaIII cell sorter (BD Biosciences).

Xenografts

All animal experiments were approved by the institutional animal care and use committee at City of Hope. Please see Supplementary Materials for procedures.

Immunohistochemistry

Immunohistochemical staining of formaldehyde-fixed, paraffin-embedded primary or xenograft tumor tissues was carried out as previously reported (14) using the following antibodies and dilutions: human CCL2 (catalog #ab9669; Abcam), 1:75 dilution; NOTCH1 (for primary breast cancer: catalog #1935-1, Epitomics; for xenograft tumors: catalog #3608, Cell Signaling), 1:40 dilution; and SMA (catalog #ab5694; Abcam), 1:100 dilution. For CCL2 and α-smooth muscle actin (SMA),

cytoplasmic staining was evaluated and for NOTCH1 nuclear staining was evaluated. Stained slides were scored according to intensity of staining (−, 0; +, 1; ++, 2; and +++, 3) and percentage of tumor cells staining positive for each antigen (0%, 0; 1%–30%, 1; 31%–70%, 2; and >70%, 3). The score for the intensity of immunostaining was multiplied by the score for the percentage of cells staining positive to obtain a final score, which was used in the statistical correlation analysis of CCL2 and NOTCH1.

Statistical analyses

All quantitative data are presented as mean ± SD. All results were confirmed in at least 3 independent experiments, and data from one representative experiment was shown. The statistical analysis was conducted with a SPSS 13.0 software package. Student *t* test or ANOVA test was used for comparison of quantitative data. Values of *P* less than 0.05 were considered significant. The differential expression of CCL2, CCR2, and NOTCH family of receptors and ligands between grade III and grade I breast cancers were analyzed using a logistic regression model after which an OR was reported. For example, an OR of 13.72 (CCL2) means that tumors with each unit increase in CCL2 expression are 13.72 times more likely to be grade III, rather than grade I [95% confidence internal (CI), 2.66–70.89]. The linear dependence between CCL2 and NOTCH1 expression was evaluated by Pearson (for the microarray data set) or Spearman correlation coefficient (for the immunohistochemical data set). The microarray gene expression data and associated clinical data were extracted from a published 295 breast cancer data set (15, 16).

Results

CAF-derived CCL2 induces the stem cell–like mammosphere-forming phenotype in breast cancer cells

The mammosphere assay has been used to functionally characterize and enrich normal and malignant stem cells from the breast, relying on the unique feature of stem cells to escape anoikis and grow into spheres in anchorage-independent conditions (17, 18). Using this approach, we examined the sphere-forming efficiency (SFE) in BT474 breast cancer cells in the presence or absence of cocultured primary human mammary NAFs or CAFs. Compared with the breast cancer cells that were cultured alone, coculture with CAFs, but not NAFs, significantly increased mammosphere formation in breast cancer cells (Fig. 1A). When NAFs and CAFs were first activated *in vitro* by coculturing with BT474 cells before being transferred to the mammosphere coculture, both activated NAFs and the CAFs that were continuously activated by breast cancer cells *in vitro* were able to induce BT474 mammosphere formation to a greater extent than their preactivation counterparts (Fig. 1A). The mammosphere-inducing effect was also observed with the conditioned medium (CM) harvested from CAFs, but not NAFs. CM from CAFs that were further activated by BT474 or MDA361 breast cancer cells exhibited an enhanced capacity for inducing mammosphere formation. *In vitro* activation of NAFs also resulted in mammosphere-inducing activity in the CM, which was more significant in NAFs that had been cocultured with BT474 cells for a prolonged 10-day period (Fig. 1B). These results indicate that the continuous activation of stromal fibroblasts by breast cancer cells leads to secretion of fibroblast-derived soluble factors that can induce the CSC-like phenotype.

To identify these soluble factors, we conducted a cytokine array assay using the CM of untreated and BT474-treated CAFs. Significant induction of CCL2 was observed following *in vitro* activation of CAFs (Fig. 1C). At the RNA level, expression of CCL2 was induced in CAFs 7- to 9-fold in response to activation by various breast cancer cells, with breast cancer–activated CAFs producing the highest amounts of CCL2 among various cell types, including NAFs and breast cancer cells. Treatment of CAFs with the noncancerous MCF10A human mammary epithelial cells, as well as short-term (3 day) treatments of NAFs with breast cancer cells only modestly induced CCL2 expression (Fig. 1D). To examine the direct effect of CCL2 on CSCs, we added increasing amounts of recombinant CCL2 to various breast cancer cells, and observed dose-dependent formation of mammospheres in BT474 and MDA361, but not MCF7 cells (Fig. 1E). Using a neutralizing antibody for CCL2, we further showed that depletion of functional CCL2 from the CM of activated CAFs abolished the CSC-inducing activity (Fig. 1F). Thus, we concluded that breast cancer–activated CAFs regulate CSCs through expression and secretion of higher levels of CCL2.

CCL2 induces the self-renewing expansion of CSCs

The sphere-initiating CSCs are maintained in the primary mammospheres through self-renewal, and are able to give rise to secondary mammospheres when cells from the primary spheres are dissociated and allowed to grow in anchorage-independent conditions (17). We therefore examined the effect of CCL2 on CSC self-renewal by secondary mammosphere culture. Interestingly, compared with the control spheres that had not been treated with CCL2, the first-passage spheres that had been treated with CCL2 contained higher numbers of CSCs capable of initiating secondary spheres, even in the absence of continuous CCL2 treatment (Fig. 2A). On the basis of this result, we hypothesized that CCL2 either promoted the self-renewal (to cause a self-renewing expansion) of existing CSCs, or, alternatively, promoted the conversion of non-CSCs to CSCs. These possibilities were examined using a reported approach involving the labeling of an initial cell population with PKH fluorescent dye and tracking the serial dilution of fluorescence in single-cell–formed spheres during the cell division events in mammosphere formation (19). Because the PKH dye binds to cell membranes and segregates in daughter cells after each cell division, the PKH fluorescence intensity of each cell in a sphere reflects its proliferation history. The PKH^{high} cells, therefore, represent the stem cell population that has undergone a limited number of divisions during sphere formation, in contrast to the nonstem, PKH^{low} cells that are highly proliferative (19). Using PKH67-labeled BT474 cells, we generated primary mammospheres containing cells with various PKH67 intensities. In the absence of CCL2 treatment, about 50% of mammospheres carried 1 $PKH67^{high}$ cell per sphere, and about 33% and 13% carried 2 and 3 $PKH67^{high}$

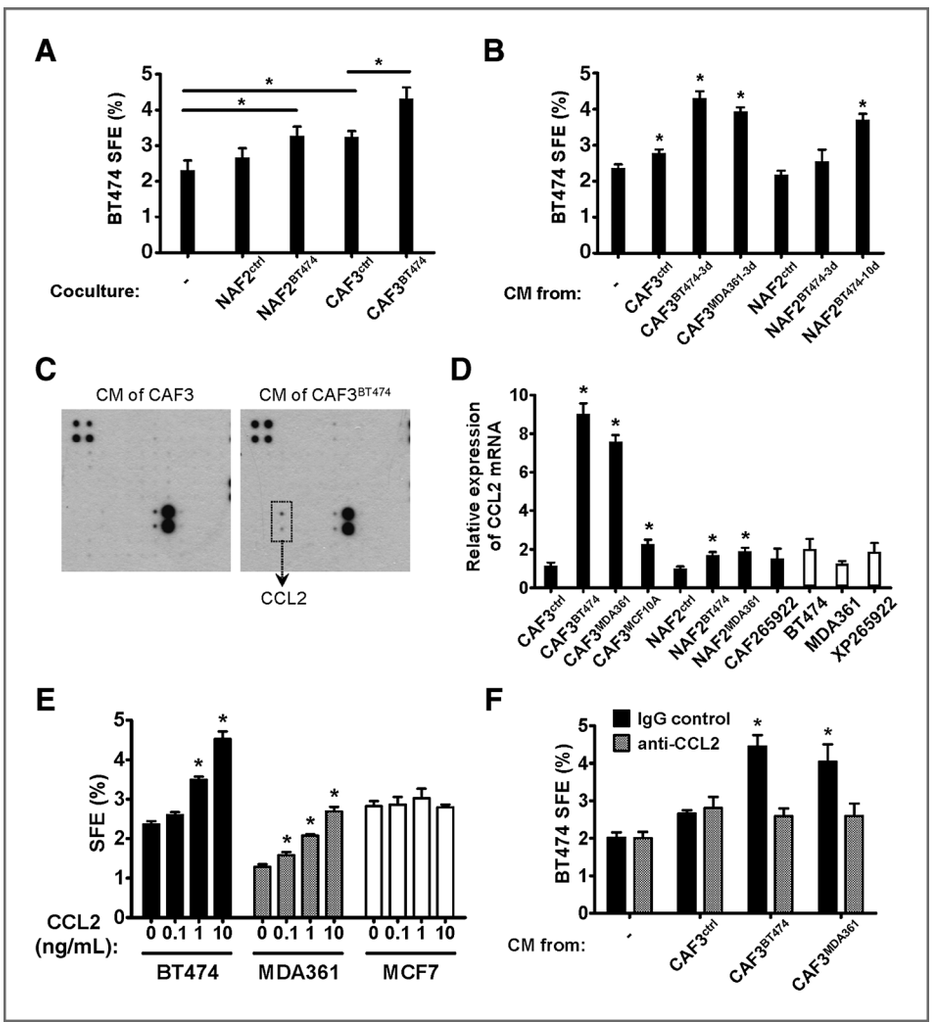

Figure 1. CCL2 secreted by cancer-activated fibroblasts induces mammosphere formation in breast cancer cells. A, mammosphere formation assay of BT474 cells cocultured with various fibroblasts. NAFs and CAFs were first cocultured with BT474 cells growing in Transwell inserts for 3 days ($NAF2^{BT474}$ and $CAF3^{BT474}$) or cultured alone ($NAF2^{ctrl}$ and $CAF3^{ctrl}$) before being transferred to Transwell inserts and cocultured with freshly plated BT474 cells for mammosphere assays. Spheres were counted on day 10, and SFE was calculated. *, $P < 0.01$. B, mammosphere formation assay of BT474 cells exposed to the conditioned media (CM) of differentially treated fibroblasts. Fibroblasts were first treated with BT474- or MDA361-derived CM for 3 or 10 days as indicated by 3d or 10d in the superscript, or with regular medium ($NAF2^{ctrl}$ and $CAF3^{ctrl}$). Treated fibroblasts were then cultured in sphere-forming media for 24 hours to prepare CM subsequently used in BT474 sphere formation assays. *, $P < 0.01$ compared with the control (the first column). C, CM was collected from CAF3 that had been previously treated for 3 days with BT474 CM ($CAF3^{BT474}$) and from untreated CAF3 as a control. Concentrated CM was subjected to a cytokine antibody array. Induction of CCL2 protein was observed in the CM of $CAF3^{BT474}$. D, relative expression of CCL2 mRNA in various cell types was determined by quantitative reverse transcription PCR (qRT-PCR). CAF265922 (primary CAFs) and XP265922 (primary tumor cells) were isolated from the same breast cancer specimen. The superscripts denote CM treatments as in B. The time length of CM treatment was 3 days in CAF3 and 10 days in NAF2. *, $P < 0.01$ compared with the untreated control CAF3 or NAF2. E, BT474, MDA361, and MCF7 breast cancer cells were assayed for sphere formation in the presence of CCL2 at the indicated concentrations. *, $P < 0.01$ compared with the control (no CCL2 treatment) in each cell line. F, effect of CAF CM (as indicated in B) on BT474 sphere formation in the presence or absence of a CCL2 neutralizing antibody. *, $P < 0.01$ compared with the control (the first column). Each bar represents the mean ± SD of 3 wells.

cells, respectively. This distribution was altered in CCL2-treated spheres, where the percentage of spheres carrying a single $PKH67^{high}$ cell decreased to 28%, and of those carrying 3 or more $PKH67^{high}$ cells significantly increased (Fig. 2B). In spheres carrying multiple $PKH67^{high}$ cells, the $PKH67^{high}$ cells also exhibited slightly dimmer fluorescence comparing to those in spheres carrying single $PKH67^{high}$ cells (Fig. 2B and Supplementary Fig. S2), likely indicating one or 2 more rounds of division (and PKH67 dilution) of the $PKH67^{high}$ cells before entering the stem cell–like, slow-proliferating or quiescent state in the multi-$PKH67^{high}$ cell spheres. The overall population of $PKH67^{high}$ cells in dissociated sphere cells was also approximately 2-fold higher in CCL2-treated spheres than untreated spheres, as determined by flow cytometric analysis (Fig. 2C). When the $PKH67^{high}$ and $PKH67^{low}$ sphere cells were purified by fluorescence-activated cell sorting, the $PKH67^{high}$

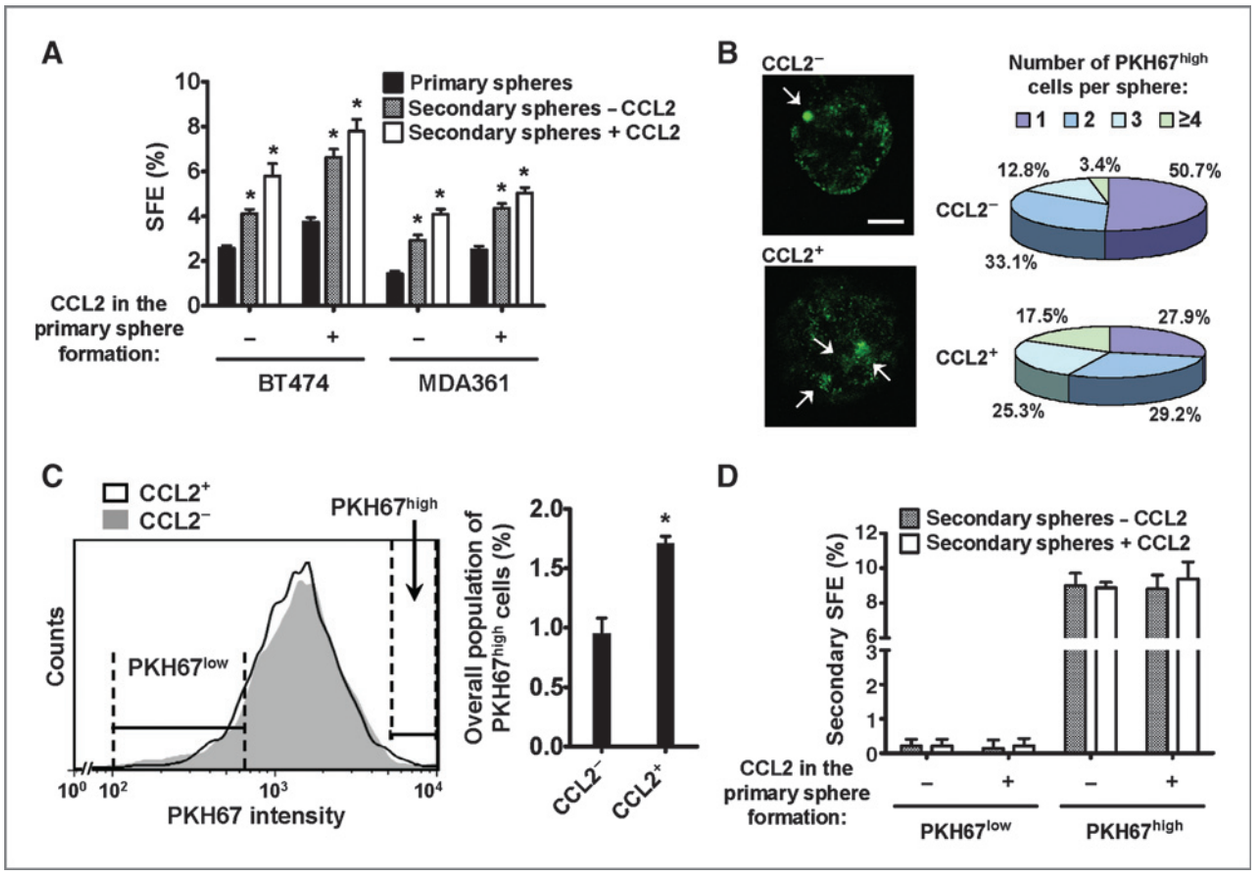

Figure 2. CCL2 induces the self-renewing expansion of CSCs. A, primary and secondary sphere formation in the presence or absence of CCL2 (10 ng/mL). *, $P < 0.01$ compared with the control (the first column in each cell line). B, left, confocal images of representative spheres formed by PKH67-labeled BT474 cells in the presence or absence of CCL2. PKH67^{high} cells are indicated by arrows. Scale bar, 20 μm. Right, summary of the numbers of PKH67^{high} cells per sphere by counting 150 spheres formed in the presence or absence of CCL2. C, a representative histogram indicating the flow cytometric profile of dissociated primary sphere cells and gating of PKH67^{low} and PKH67^{high} cells. Percentage of PKH67^{high} cells was summarized in the bar graph. Each bar represents the mean ± SD of 3 independently treated sphere cultures. *, $P < 0.01$. D, secondary mammosphere formation of sorted PKH67^{high} and PKH67^{low} primary sphere cells. Each bar represents the mean ± SD of 3 wells.

primary sphere cells exhibited the highest SFE in the secondary mammosphere formation assay when compared with the PKH67^{low} cells (Fig. 2D), consistent with their CSC property. CCL2 treatment did not alter the SFE of PKH67^{low} and PKH67^{high} cells in the secondary sphere formation (Fig. 2D), indicating that CCL2 does not cause conversion of non-CSCs (PKH67^{low}) to CSCs (sphere initiating). Therefore, we conclude that CCL2 regulates CSCs by inducing their self-renewing expansion. Interestingly, a similar effect has been previously described for NOTCH activation on stem cells (8). The role of NOTCH pathway in mediating CSC regulation by CCL2 was further investigated in Fig. 4.

Paracrine signaling of cancer-secreted cytokines induces CCL2 production in fibroblasts via STAT3 activation

We then set out to identify the mechanism underlying increased CCL2 production in breast cancer–activated CAFs. STAT3 has been recently reported to bind to and activate the promoter of *CCL2* (20). To determine whether breast cancer cells induce CCL2 expression in fibroblasts through STAT3 activation, we first examined the effects of breast cancer–derived CM and a STAT3 inhibitor on a previously reported *CCL2* promoter reporter (21) and on CCL2 expression in CAFs freshly isolated from a triple-negative (ER$^-$/PR$^-$/HER2$^-$) primary breast cancer (CAF265922). CM from breast cancer cells, including BT474, MDA361, and the primary breast cancer cells isolated from the same breast cancer specimen (XP265922), but not from MCF10A cells, markedly induced luciferase expression driven by the *CCL2* promoter (Fig. 3A), as well as endogenous expression of CCL2 (Fig. 3B). These effects were abrogated by addition of the STAT3 inhibitor (Fig. 3A and B), indicating STAT3 involvement in mediating the induction of fibroblast-derived CCL2 expression. Similar results were also obtained using CAFs from a different primary breast cancer (Supplementary Fig. S3). Indeed, high levels of STAT3 phosphorylation were observed in CAFs as early as 30 minutes following treatment with breast cancer–derived, but not MCF10A-derived, CM (Fig. 3C). The induction of CCL2 expression was sustained over a time course of 5 days in CAFs cocultured with breast cancer cells, and was abolished by

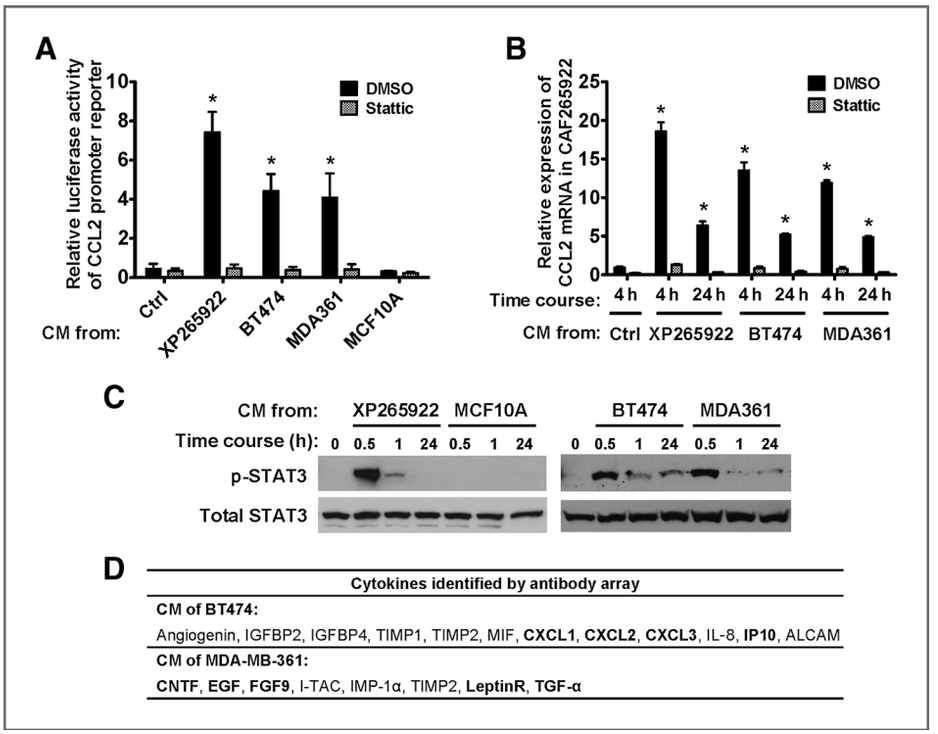

Figure 3. Paracrine signaling of cancer-secreted cytokines induces CCL2 production in fibroblasts via STAT3 activation. A, a luciferase reporter containing a 2.8-kb CCL2 promoter was transfected into CAF265922 cells. Luciferase activity was analyzed at 4 hours after CM exposure in the presence of dimethyl sulfoxide (DMSO) or Stattic (a STAT3 inhibitor; 5 μmol/L). Each bar represents the mean ± SD of 3 independently transfected wells. *, $P < 0.01$ compared with the control (the first column). B, total RNA isolated from CAF265922 that had been treated with CM from indicated breast cancer cells for 4 or 24 hours was analyzed for CCL2 mRNA level by qRT-PCR. Data were normalized to 18S in each sample. Each bar represents the mean ± SD of 3 wells. *, $P < 0.01$ compared with the control (the first column). C, CAF265922 cells were treated with CM from indicated cells and analyzed by Western blotting. D, summary of the cytokine array data identifying cytokines constitutively secreted by BT474 and MDA361 breast cancer cells. Cytokines that are known to activate STAT3 are in bold.

inhibition of STAT3 (Supplementary Fig. S4). Although CM from BT474, MDA361, and primary breast cancer cells all induced STAT3 phosphorylation and CCL2 expression in CAFs, different cytokines were detected in the CM of BT474 and MDA361 (Fig. 3D). In either case, multiple cytokines with reported STAT3-activating effect were detected, suggesting that the STAT3 activation observed in breast cancer–treated CAFs was likely a combined effect of various breast cancer–secreted cytokines. Thus, breast cancer cells derived from different origins and secreting different cytokines activate the STAT3 core pathway in fibroblasts of the tumor microenvironment, leading to STAT3-mediated promoter activation of *CCL2*.

CCL2 induces CSCs by activating NOTCH signaling

To explore the molecular basis for CCL2-mediated regulation of CSCs, we surveyed the CCL2 responsiveness of genes involved in NOTCH, Wnt/β-catenin and Hedgehog pathways, which are known to regulate stem cells (8, 22, 23). We found that expression of NOTCH1 and a target gene of NOTCH signaling, HES1, were induced by CCL2 in various breast cancer cells, and that HES1 expression occurred subsequent to NOTCH1 expression (Fig. 4A and B). Interestingly, the NOTCH-activating effect of CCL2 was only subtle in MCF7 cells, which also failed to respond to CCL2-induced sphere formation (Fig. 1E). This may be related to the lower expression level of CCR2 in MCF7 than in other cells (Supplementary Fig. S5), making MCF7 less sensitive to CCL2-triggered effects. Transfected HES1 and HEY1 reporters were significantly activated by CCL2 in primary breast cancer cells and BT474 cells, and these effects were abolished by inhibitors of the NOTCH-activating α- and γ-secretases (Fig. 4C and Supplementary Fig. S6). Activation of NOTCH signaling by CCL2 was thus attributed to increased NOTCH1 expression, as CCL2 showed no effect on the activities of α- and γ-secretases as assessed by *in vitro* substrate cleavage assays (Supplementary Fig. S7). Upon CCL2 treatment, a rapid and dramatic induction of p38 MAPK phosphorylation was observed, followed by the induction of NOTCH1 and NICD1 (cleaved NOTCH1) proteins at a later time point (Fig. 4D). Both p38 phosphorylation and NOTCH1/NICD1 induction were abolished by an inhibitor of p38 MAPK (Fig. 4D and E). Using a 6-kb *NOTCH1* promoter reporter, we observed an approximately 4-fold induction of *NOTCH1* promoter activity by CCL2 in primary breast cancer cells, and this effect was also completely suppressed by the p38 MAPK inhibitor, but only partially suppressed by inhibitors of phosphoinositide 3-kinase (PI3K) and MAP–ERK kinase (MEK)1/2 MAPK (Fig. 4F). This suggests that p38 MAPK plays an essential role in activating *NOTCH1* promoter, whereas PI3K and MEK1/2 MAPK may play an accessory role. Induction of p38

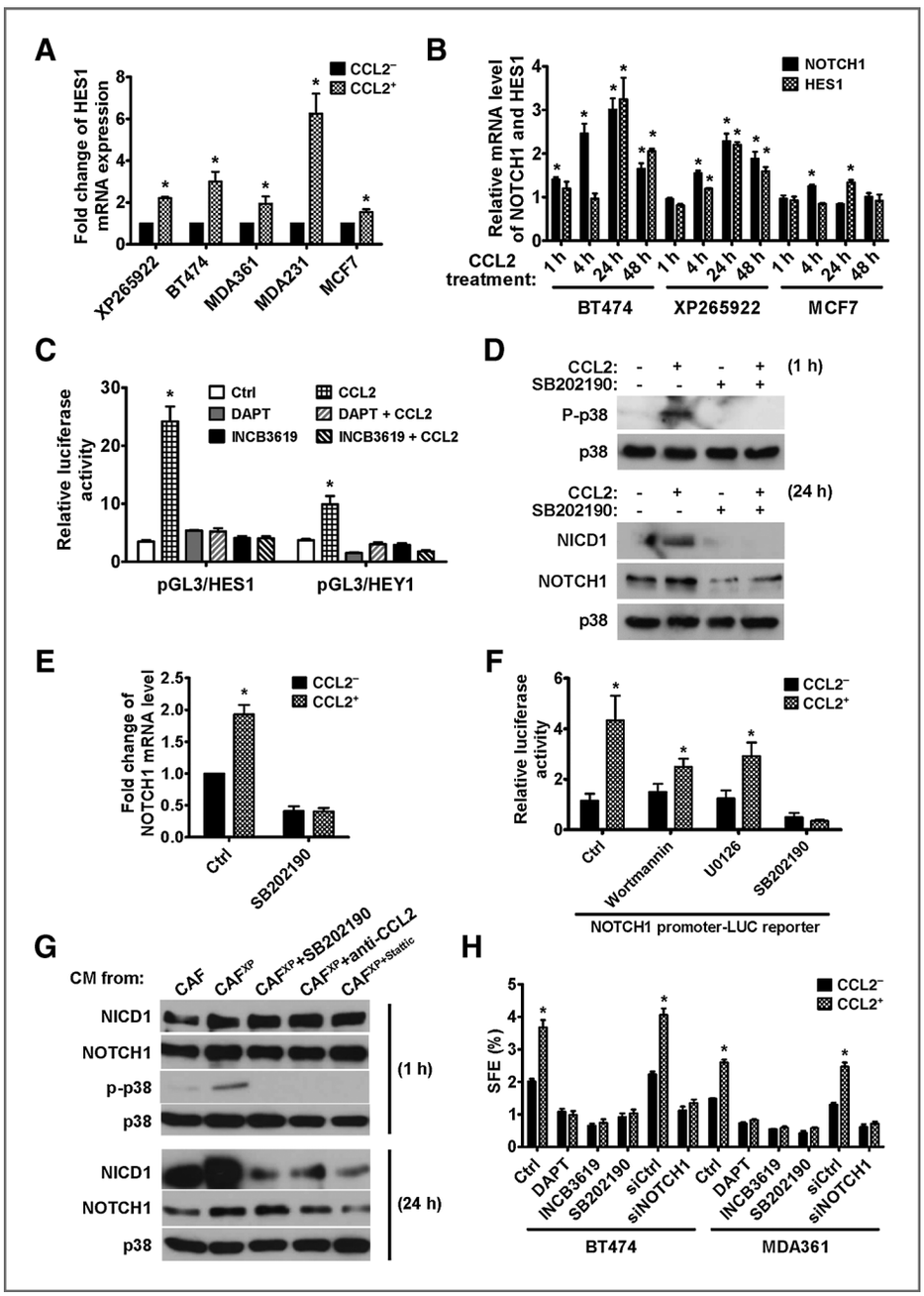

Figure 4. CCL2 regulates CSC phenotype in breast cancer cells by activating NOTCH signaling. A, total RNA isolated from various breast cancer cell lines treated with CCL2 or vehicle for 24 hours were analyzed for the expression of HES1, a target gene activated by NOTCH signaling. Data of qRT-PCR were normalized to 18S in each sample. Each bar represents the mean ± SD of 3 wells. *, $P < 0.001$ compared with the control (the first column). B, expression of NOTCH1 and HES1 mRNAs upon CCL2 treatment in the indicated time course. The mRNA level at each time point was compared with that in untreated cells, which was set as 1. Each bar represents the mean ± SD of 3 wells. *, $P < 0.01$ compared with untreated cells. C, luciferase reporters of HES1 and HEY1 were transfected into XP265922 primary breast cancer cells. Luciferase activity was analyzed at 24 hours post-CCL2 treatment ± inhibitors of γ-secretase (DAPT; 10 μmol/L) or α-secretase (INCB3619; 5 μmol/L). Each bar represents the mean ± SD of 3 independently transfected wells. *, $P < 0.001$ compared with the control (the first column). D, Western blot analysis of p38 and NOTCH1 at indicated time points following treatment conditions in XP265922 cells. E, expression of NOTCH1 mRNA in XP265922 cells treated with CCL2 ± SB202190 (5 μmol/L) for 24 hours. *, $P < 0.001$ compared with the control (the first column). F, a luciferase reporter containing a 6-kb NOTCH1 promoter was transfected into XP265922 cells to analyze NOTCH1 promoter regulation by CCL2 and various inhibitors (Wortmannin, 1 μmol/L; U0126, 10 μmol/L; SB202190, 5 μmol/L). Each bar represents the mean ± SD of 3 independently transfected wells. *, $P < 0.001$ compared with the control (the first column). G, XP265922 cells were treated with CM from indicated sources and analyzed for NOTCH1 and p38 expression by Western blotting. H, mammosphere formation assay of breast cancer cells treated with various inhibitors in the presence or absence of CCL2. Each bar represents the mean ± SD of 3 wells. *, $P < 0.01$ compared with the control (the first column in each cell line).

MAPK phosphorylation and NOTCH1 proteins (full-length and cleaved) was also observed in XP265922 breast cancer cells treated with CM from CAF265922 previously activated by coculturing with XP265922. This effect was abolished by treatment with a p38 MAPK inhibitor or CCL2 neutralizing antibody, and also by using CM from CAF265922 previously cocultured with XP265922 cells but in the presence of a STAT3 inhibitor (Fig. 4G). We therefore concluded that in breast cancer cells, CCL2 induces NOTCH1 expression and its downstream signaling mainly through p38-dependent activation of the *NOTCH1* promoter. In BT474 and MDA361 breast cancer cells, CCL2-induced mammosphere formation was efficiently blocked by inhibitors of the α- and γ-secretases and p38 MAPK, and by RNA interference (RNAi) of NOTCH1 (Fig. 4H), indicating that activation of NOTCH1 mediates the effect of CCL2 on CSCs.

Fibroblast-specific knockdown of CCL2 or CCL2 depletion by a neutralizing antibody inhibits *in vivo* tumorigenesis

To obtain *in vivo* evidence of the CSC-regulating function of fibroblast-derived CCL2, we established an orthotopic xenograft model of cotransplanted primary CAFs and breast cancer cells. CAF265922 were stably transduced to express doxycycline-inducible shRNA of CCL2, which suppressed CCL2 expression *in vitro* by approximately 60% in the presence of doxycycline (Fig. 5A). The modified CAFs were then cotransplanted with breast cancer cells from the same primary tumor (XP265922) into the mammary fat pads of female NOD/SCID/IL-2Rγ-null (NSG) mice. Mammary tumor formation was monitored in transplanted mice with or without doxycycline treatment. Fibroblast-specific knockdown of CCL2 in the doxycycline $(Dox)^+$ group resulted in significantly delayed tumor formation and reduced tumor volume, compared with the Dox^- control group (Fig. 5B and C). Xenograft tumors from both groups were harvested, and the fibroblast (labeled by lentiviral-encoded GFP) and tumor cell (positive for human ESA) components were separated for gene expression analyses. In Dox^+ tumors, both fibroblast-derived CCL2 expression and tumor cell–derived NOTCH1 expression were significantly lower than their counterparts in Dox^- tumors (Fig. 5D). Immunohistochemical staining also indicated lower levels of CCL2 and NOTCH1 proteins in the Dox^+ tumors than in the Dox^- tumors (Fig. 5E). We further analyzed the CSC population within all tumor cells in each xenograft tumor using ALDEFLUOR flow cytometric analysis. The $ALDEFLUOR^{bright}$ CSC populations in Dox^+ tumors were significantly smaller than those in Dox^- tumors (Fig. 5F; ∼0.45% vs. ∼1.3%), indicating a decrease in the number of CSCs. Thus, fibroblast-derived CCL2 secretion appears to play an important role in tumorigenesis and in regulating NOTCH1 expression and the CSC population in breast cancer cells. Consistent with these results, the CCL2 neutralizing antibody, but not a control IgG or PBS, significantly suppressed tumorigenesis and decreased NOTCH1 expression in tumor cells when XP265922 and GFP-labeled CAF265922 were cotransplanted into NSG mice (Fig. 5G and H and Supplementary Fig. S8). Thus, based on the studies that have been described to this point, we propose a model of CSC generation that incorporates a cross-talk circuit involving STAT3, CCL2, and NOTCH pathways (Fig. 5I).

Expression of CCL2 and NOTCH1 are correlated in primary breast cancers and associated with poor differentiation of tumor cells

To extend our findings to a larger number of primary breast cancers, OR and 95% CI were calculated using unconditional logistic regression to determine whether the microarray-determined expression levels of CCL2, CCR2, and NOTCH family of receptors and ligands in a previously reported breast cancer data set (15, 16) were associated with tumor grade (Table 1). Patients with grade III (poorly differentiated) and grade I (well-differentiated) tumors were included in the analysis. We did not include the grade II tumors because they fell between grade I and grade III and exhibited highly diverse levels of differentiation than grades I and III. Patients with poor differentiation (grade III) were significantly associated with higher levels of CCL2 (OR, 13.72; 95% CI, 2.66–70.89), NOTCH1 (OR, 9.56; 95% CI, 1.54–59.27), and delta-like 3 (OR, 20.93; 95% CI, 1.53–289.94), as well as lower level of Jagged 1 (OR, 0.14; 95% CI, 0.03–0.57).

In addition, correlation coefficients were calculated between microarray-determined CCL2 and NOTCH1 expression and stratified by tumor grade and stage (Table 2, microarray-based expression). A significant linear correlation was observed between CCL2 and NOTCH1 expression among all breast cancers ($R = 0.18$, $P < 0.01$). This association was especially pronounced in grade III tumors ($R = 0.19$, $P = 0.03$), and in Stage I ($R = 0.33$, $P < 0.01$) and Stage IIa disease ($R = 0.19$, $P = 0.02$). We further evaluated the expression of CCL2 and NOTCH1 at the protein level by immunohistochemistry in 51 $HER2^+$ or triple-negative primary breast cancers. The correlation between 2 proteins was approaching statistical significance ($R = 0.26$, $P = 0.06$) among all tumors, and was indeed significant within $HER2^+$ tumors ($R = 0.40$, $P = 0.03$), but not triple-negative breast cancers (Table 2, immunohistochemistry-based expression). Although the previously reported association of CCL2 with poor clinical outcome (24) was not detected in the current cohort, our results nevertheless support a relationship between CCL2 and NOTCH1 with effects on CSCs in primary breast cancers.

Discussion

Fibroblasts are altered by cancer cells through nongenetic modifications, and in turn, effect direct changes on cancer cells or indirect changes on the tumor microenvironment to facilitate cancer growth and invasion. The resulting coevolution of cancer and the hosting niche critically influences disease progression. Our attention to the influence of fibroblasts on CSCs, the seeds of cancer, showed that, upon cancer-mediated activation, human mammary fibroblasts secreted CCL2 to induce CSC generation through activation of NOTCH signaling. In the cancer niche, CCL2 may be produced and secreted into the extracellular environment by almost all cell types, including cancer cells, stromal fibroblasts, tumor-infiltrated monocytes, and endothelial cells. Nevertheless, our study indicated that (i) CCL2 expression was 4- to 9-fold higher in activated CAFs than in breast cancer cells (Fig. 1D);

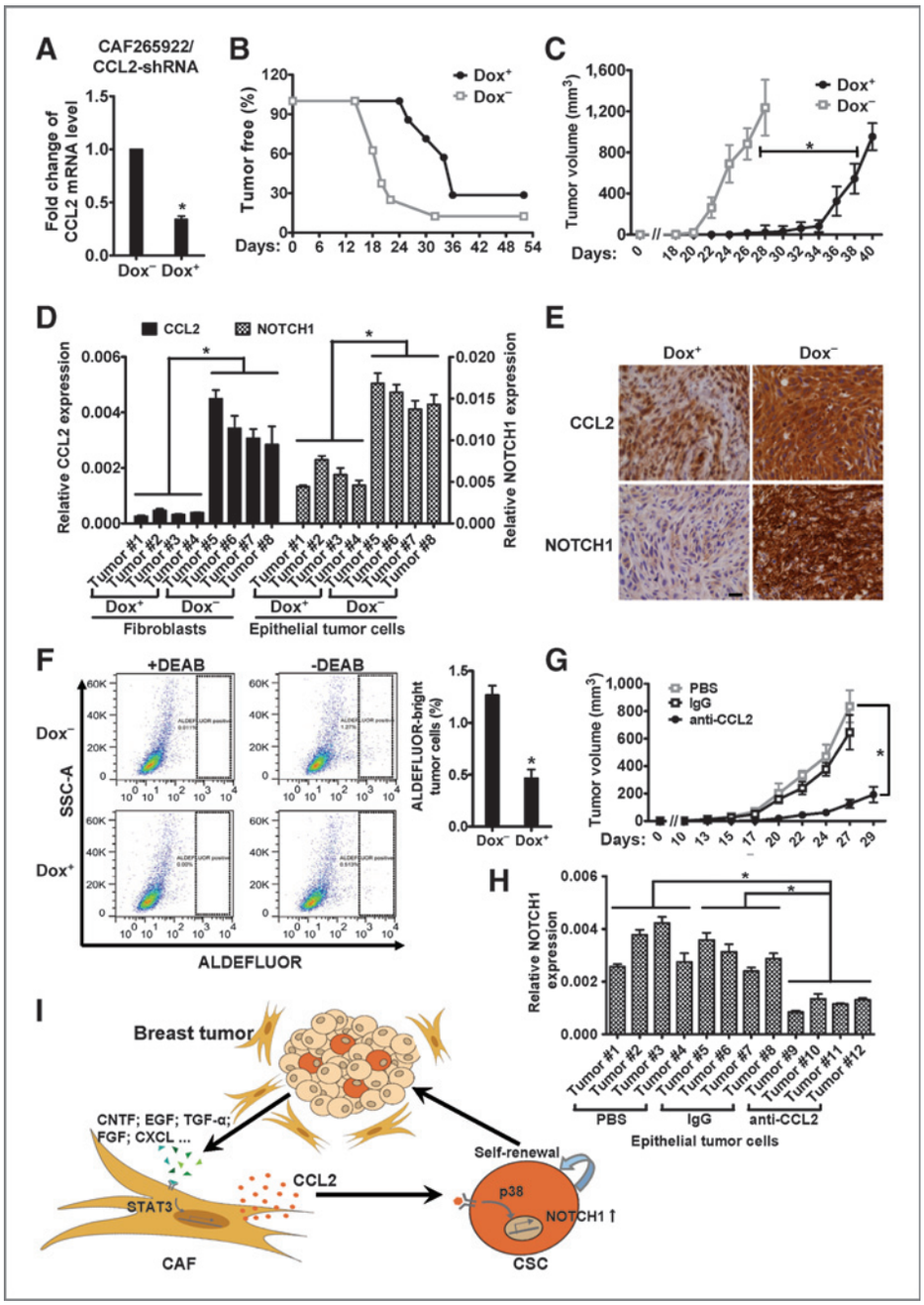

Figure 5. Fibroblast-specific CCL2 knockdown or CCL2 depletion by neutralizing antibody inhibits *in vivo* tumorigenesis. A, CAF265922 cells stably expressing doxycycline-inducible CCL2 shRNA were examined for CCL2 mRNA expression by qRT-PCR upon 48 hours treatment of doxycycline (1 μg/mL) or vehicle. *, $P < 0.001$. B, *in vivo* tumor formation was examined by cotransplanting unmodified XP265922 primary breast cancer cells and the CAF265922 cells tested in A into the mammary fat pads of NOD/SCID/IL-2Rγ-null mice, as described in Materials and Methods. The time course of xenograft tumor formation in doxycycline-treated mice (Dox^+) and control mice (Dox^-) was compared. $P < 0.001$ between the 2 groups. C, tumor volume determined in Dox^+ and Dox^- mice. *, $P < 0.001$ at each available time point starting from day 22. D, total RNA was isolated from fibroblasts and epithelial tumor cells purified from the Dox^+ and Dox^- xenograft tumors, and subjected to qRT-PCR for CCL2 and NOTCH1 expression, respectively. *, $P < 0.001$. E, representative immunohistochemical images of Dox^+ and Dox^- xenograft tumor sections stained with antibodies against CCL2 and NOTCH1 (×40; bar, 20 μm). F, representative flow cytometric dot plots indicating the ALDEFLUOR-bright tumor cells from Dox^+ and Dox^- xenograft tumors. Diethylaminobenzaldehyde (DEAB), an inhibitor of ALDH, was added in the left 2 panels. Bar graph, averaged percentages of the ALDEFLUOR-bright population from bulk tumor cells in 4 Dox^+ and 4 Dox^- xenograft tumors. *, $P < 0.001$. G, tumor volume determined in mice treated with PBS, IgG, or CCL2 neutralizing antibody. *, $P < 0.001$. H, total RNA was isolated from epithelial tumor cells purified from the 3 groups of xenograft tumors and subjected to qRT-PCR for NOTCH1 expression. *, $P < 0.001$. I, a model of the CSC-stimulating cross-talk circuit that involves STAT3, CCL2, and NOTCH pathways. In the tumor microenvironment, paracrine signaling initiated by breast cancer cells induces CCL2 production by stromal fibroblasts through STAT3 activation, and the fibroblast-derived CCL2, in turn, promotes cancer progression by regulating CSCs through activation of the NOTCH pathway.

Table 1. Relative odds of having breast cancer grade III (N = 119) versus grade I (N = 75) associated with CCL2- and NOTCH-related genes

Gene symbol	Gene name	OR[a] (95% CI)	*P*
CCL2	Chemokine (C-C motif) ligand	**13.72 (2.66–70.89)**	**<0.01**
CCR2	Chemokine (C-C motif) receptor	6.32 (0.87–45.82)	0.07
NOTCH1	Notch homolog 1	**9.56 (1.54–59.27)**	**0.02**
NOTCH2	Notch homolog 2	0.76 (0.15–3.90)	0.74
NOTCH3	Notch homolog 3	2.51 (0.36–17.29)	0.35
NOTCH4	Notch homolog 4	0.39 (0.03–4.33)	0.44
DLL1	Delta-like 1	0.48 (0.10–2.30)	0.36
DLL3	Delta-like 3	**20.93 (1.53–286.94)**	**0.02**
DLL4	Delta-like 4	1.16 (0.03–49.36)	0.94
JAG1	Jagged 1	**0.14 (0.03–0.57)**	**<0.01**
JAG2	Jagged 2	0.31 (0.08–1.19)	0.09

NOTE: Values in bold are statistically significant ($P < 0.05$).
[a]OR of grade III versus grade I.

(ii) fibroblast-specific knockdown of CCL2 significantly suppressed tumorigenesis and the CSC population in xenograft tumors (Fig. 5A–F); and (iii) CCL2 is detected by immunohistochemistry in both tumor cells and stromal fibroblasts in primary breast cancer (Supplementary Fig. S9). These data strongly suggest that CAFs are an important source of CCL2 in the cancer niche and a major environmental regulator of CSCs.

The CAF populations in tumor-associated stroma are known to include both fibroblasts and myofibroblasts. Myofibroblasts are endowed with the ability to promote tumor growth and associated with higher grade malignancy and poor prognosis in patients with cancer (25, 26). These cells express SMA to be distinguished from fibroblasts. Kojima and colleagues recently show that through self-sustaining autocrine signaling of TGF-β and stromal cell-derived factor-1, fibroblasts can transdifferentiate into myofibroblasts during tumor progression (26). The CAFs prepared and examined in our study indeed contained a subpopulation of SMA-expressing myofibroblasts, as indicated by immunofluorescent assay and immunohistochemistry (Supplementary Figs. S1B and S8). However, the SMA^+ myofibroblasts and SMA^- fibroblasts produced CCL2 at comparable levels in the cancer niche (Supplementary Fig. S8), suggesting that the increased CCL2 production and enhanced CSC-promoting capacity of the herein examined CAFs are unlikely related to the myofibroblast phenotype, but rather a general alteration in fibroblasts in response to cancer-derived stimulation. Our findings also support further studies on the regulation of CSCs and their noncancerous counterparts by other physiologic and therapeutic conditions that locally elevate CCL2 levels. Such conditions, including wound healing, inflammation, and chemotherapy (7, 27), are becoming increasingly appreciated for their relevance to the biology of normal and cancerous stem cells.

Table 2. Correlation between CCL2 and NOTCH1 in primary human breast cancer

Microarray-based expression

Group	*n* (%)	*R*[a]	*P*
All	**295 (100)**	**0.18**	**<0.01**
Grade			
I	75 (25.4)	0.21	0.07
II	101 (34.2)	0.02	0.81
III	**119 (40.3)**	**0.19**	**0.03**
Stage			
I	**82 (27.8)**	**0.33**	**<0.01**
IIa	**142 (48.1)**	**0.19**	**0.02**
IIb	41 (13.9)	0.05	0.76
III–IV	30 (10.2)	0.13	0.49

Immunohistochemical-based expression

Group	*n* (%)	*R*[b]	*P*
All	51 (100)	0.26	0.06
Subtype			
Triple negative	20 (39.2)	0.04	0.86
$HER2^+$	**31 (60.8)**	**0.40**	**0.03**

NOTE: Values in bold are statistically significant ($P < 0.05$).
[a]Pearson correlation coefficient.
[b]Spearman correlation coefficient.

Our data indicate that the CCL2-producing and CSC-promoting ability of CAFs is conferred by breast cancer–secreted soluble factors present in the CM, such as the cytokines listed in Fig. 3D. Although different breast cancer cells appeared to secrete distinct sets of cytokines to induce CCL2 production in CAFs, these cytokines ultimately functioned through STAT3, and inhibition of STAT3 completely abrogated the induction of CCL2 by breast cancer paracrine signaling (Fig. 3). Therefore, compared with the diverse signals released by cancer cells, the common effector STAT3 serves as a superior target to therapeutically block cancer-induced activation of stromal fibroblasts. STAT3 has been identified as an important effector and target in cancer cells and tumor-infiltrated immune cells (28).

Our study now identifies STAT3-mediated fibroblast activation as a potential therapeutic target, further supporting the idea that anti-STAT3 therapies may exert dual effects on both cancer and host cells, halting their dynamic and mutual activation during cancer progression.

CCL2 has been implicated in breast cancer progression and metastasis (29). In primary breast tumors, CCL2 expression is correlated with the accumulation of tumor-associated macrophages and is a significant indicator of early relapse (24, 30). Overexpression of CCL2 in breast cancer cells promotes metastasis formation in lungs and bone through increasing macrophage infiltration and osteoclast differentiation, respectively (31). A recent report shows that CCL2 produced by both tumor and stromal cells recruits the CCR2-expressing inflammatory monocytes to the pulmonary metastases of mammary tumors, where monocyte-derived factors promote endothelial permeability and extravasation of tumor cells (32). CCL2 expression is interactively regulated in the cross-talk between tumor and niche cells. Increased expression of CCL2 is detected in the bone marrow mesenchymal stem cells (MSC) following stimulation by leukemia cells, resulting in enhanced cancer-promoting capacity of MSCs (33). Coculture with MSCs, in turn, induces CCL2 expression in cancer cells (34). These previous studies have therefore established an important role of CCL2 in cancer–host cross-talk through the regulation of tumor cell homing and metastasis, angiogenesis, and the immune system.

Here, we show that CCL2 induces CSCs both *in vitro* and *in vivo* through activation of NOTCH (Figs. 4 and 5). NOTCH activation has been shown to promote the self-renewal of mammary stem cells (8). An important role for NOTCH signaling in human cancers has been long established (35), and several GSIs are currently in early clinical development as potential NOTCH-targeting therapeutics. It is proposed that single-agent GSI therapy may be effective in triple-negative breast cancers, which are known to harbor CSC-like characteristics (36). Here, our data further support the use of NOTCH-targeting agents in efficiently blocking the stimulatory effect of stromal fibroblasts on CSCs. Our data also indicate that activation of p38 MAPK is required for CCL2-induced NOTCH1 expression (Fig. 4). The E2A-encoded transcription factors E12 and E47 have been shown to activate NOTCH1 expression through binding to multiple E-box sites in the 6-kb *NOTCH1* promoter region (37). Phosphorylation of E47 by p38 MAPK and by MAPK-activated protein kinase 2 (MAPKAPK2), a kinase activated by p38, has been reported (38, 39). The function of p38-mediated E47 phosphorylation in regulating NOTCH1 promoter activity is still unclear, and may underlie the induction of NOTCH1 by CCL2, which induces potent p38 activation in primary breast cancer cells (Fig. 4D). In addition, the NOTCH-activating effect of CCL2 was only subtle in the $ER^+/PR^+/HER2^-$ MCF7 cells (Fig. 4A and B), which also failed to respond to CCL2-induced sphere formation (Fig. 1E). Whether the lower CCR2 level in MCF7 (Supplementary Fig. S5) causes their low sensitivity to CCL2 effect, and whether levels of CCL2 receptors are associated with breast cancer subtypes need to be further investigated. Nevertheless, immunohistochemical staining of primary breast cancers indicated a significant correlation between CCL2 and NOTCH1 in $HER2^+$ tumors (Table 2, immunohistochemistry-based expression), suggesting that at least in these tumors, as observed in the $HER2^+$ BT474 and MDA361 breast cancer cells, the regulation of NOTCH signaling by CCL2 may indeed occur *in vivo*.

In summary, our study provides a model in which paracrine signaling initiated by breast cancer cells induces CCL2 production by stromal fibroblasts through STAT3 activation. The fibroblast-derived CCL2, in turn, promotes cancer progression by regulating CSCs through NOTCH activation (Fig. 5I). The results described herein provide novel insights into understanding how CSCs are influenced by the tumor microenvironment during the coevolution of cancer and the hosting niche, and identify CCL2, STAT3, and NOTCH1 as future therapeutic targets to efficiently block the CSC-stimulating cancer–host cross-talk to overcome CSC-mediated disease progression and treatment resistance.

Disclosure of Potential Conflicts of Interest

T. Luu has commercial research support from NCI/CTEP, Bayer/Onyx, Wyth, Merk, BMS, GSK, and Pfizer and is the consultant/advisory board member for Novartis and Genomic Health. No potential conflicts of interest were disclosed by the other authors.

Acknowledgments

The authors thank Drs. Leonid S. Metelitsa and Warren S. Pear for kindly providing the plasmid constructs of *CCL2* and *NOTCH1* promoter reporters; Drs. John J. Rossi and Hua Yu for providing reagents, Drs. Susan Kane, Mei Kong, Toshifumi Tomoda, and Takahiro Maeda and members of the Division of Tumor Cell Biology for valuable comments, as well as the Analytical Cytometry Core, Light Microscopy Digital Imaging Core, Bioinformatics Core, Biostatistics Core, Pathology Core, and Animal Facility for professional services.

Grant Support

The project described was supported by the National Cancer Institute (NCI) grant number R00 CA125892 (S.E. Wang) and P30 CA033572, and by the National Natural Science Foundation of China grant number 30872986 (X. Ren) and 81171983 (H. Li).

The costs of publication of this article were defrayed in part by the payment of page charges. This article must therefore be hereby marked *advertisement* in accordance with 18 U.S.C. Section 1734 solely to indicate this fact.

Received October 28, 2011; revised February 20, 2012; accepted March 18, 2012; published OnlineFirst April 3, 2012.

References

1. Visvader JE, Lindeman GJ. Cancer stem cells in solid tumours: accumulating evidence and unresolved questions. Nat Rev Cancer 2008;8:755–68.
2. Ailles LE, Weissman IL. Cancer stem cells in solid tumors. Curr Opin Biotechnol 2007;18:460–6.
3. Kalluri R, Zeisberg M. Fibroblasts in cancer. Nat Rev Cancer 2006;6:392–401.
4. Kuperwasser C, Chavarria T, Wu M, Magrane G, Gray JW, Carey L, et al. Reconstruction of functionally normal and malignant human breast tissues in mice. Proc Natl Acad Sci U S A 2004;101:4966–71.
5. Melgarejo E, Medina MA, Sanchez-Jimenez F, Urdiales JL. Monocyte chemoattractant protein-1: a key mediator in inflammatory processes. Int J Biochem Cell Biol 2009;41:998–1001.

6. Strieter RM, Wiggins R, Phan SH, Wharram BL, Showell HJ, Remick DG, et al. Monocyte chemotactic protein gene expression by cytokine-treated human fibroblasts and endothelial cells. Biochem Biophys Res Commun 1989;162:694–700.
7. Lazennec G, Richmond A. Chemokines and chemokine receptors: new insights into cancer-related inflammation. Trends Mol Med 2010;16: 133–44.
8. Dontu G, Jackson KW, McNicholas E, Kawamura MJ, Abdallah WM, Wicha MS. Role of Notch signaling in cell-fate determination of human mammary stem/progenitor cells. Breast Cancer Res 2004;6:R605–15.
9. Lobo NA, Shimono Y, Qian D, Clarke MF. The biology of cancer stem cells. Annu Rev Cell Dev Biol 2007;23:675–99.
10. Kadesch T. Notch signaling: a dance of proteins changing partners. Exp Cell Res 2000;260:1–8.
11. Ghebeh H, Tulbah A, Mohammed S, Elkum N, Bin Amer SM, Al-Tweigeri T, et al. Expression of B7-H1 in breast cancer patients is strongly associated with high proliferative Ki-67-expressing tumor cells. Int J Cancer 2007;121:751–8.
12. Aagaard L, Amarzguioui M, Sun G, Santos LC, Ehsani A, Prydz H, et al. A facile lentiviral vector system for expression of doxycycline-inducible shRNAs: knockdown of the pre-miRNA processing enzyme Drosha. Mol Ther 2007;15:938–45.
13. Wang Y, Yu Y, Tsuyada A, Ren X, Wu X, Stubblefield K, et al. Transforming growth factor-beta regulates the sphere-initiating stem cell-like feature in breast cancer through miRNA-181 and ATM. Oncogene 2011;30:1470–80.
14. Gu L, Lau SK, Loera S, Somlo G, Kane SE. Protein kinase A activation confers resistance to trastuzumab in human breast cancer cell lines. Clin Cancer Res 2009;15:7196–206.
15. van de Vijver MJ, He YD, van't Veer LJ, Dai H, Hart AA, Voskuil DW, et al. A gene-expression signature as a predictor of survival in breast cancer. N Engl J Med 2002;347:1999–2009.
16. Chang HY, Nuyten DS, Sneddon JB, Hastie T, Tibshirani R, Sørlie T, et al. Robustness, scalability, and integration of a wound-response gene expression signature in predicting breast cancer survival. Proc Natl Acad Sci U S A 2005;102:3738–43.
17. Dontu G, Abdallah WM, Foley JM, Jackson KW, Clarke MF, Kawamura MJ, et al. *In vitro* propagation and transcriptional profiling of human mammary stem/progenitor cells. Genes Dev 2003;17:1253–70.
18. Scheel C, Eaton EN, Li SH, Chaffer CL, Reinhardt F, Kah KJ, et al. Paracrine and autocrine signals induce and maintain mesenchymal and stem cell States in the breast. Cell 2011;145:926–40.
19. Cicalese A, Bonizzi G, Pasi CE, Faretta M, Ronzoni S, Giulini B, et al. The tumor suppressor p53 regulates polarity of self-renewing divisions in mammary stem cells. Cell 2009;138:1083–95.
20. Potula HS, Wang D, Quyen DV, Singh NK, Kundumani-Sridharan V, et al. Src-dependent STAT-3-mediated expression of monocyte chemoattractant protein-1 is required for 15(S)-hydroxyeicosatetraenoic acid-induced vascular smooth muscle cell migration. J Biol Chem 2009;284:31142–55.
21. Song L, Ara T, Wu HW, Woo CW, Reynolds CP, Seeger RC, et al. Oncogene MYCN regulates localization of NKT cells to the site of disease in neuroblastoma. J Clin Invest 2007;117:2702–12.
22. Liu Y, Elf SE, Miyata Y, Sashida G, Liu Y, Huang G, et al. p53 regulates hematopoietic stem cell quiescence. Cell Stem Cell 2009;4:37–48.
23. Peacock CD, Wang Q, Gesell GS, Corcoran-Schwartz IM, Jones E, Kim J, et al. Hedgehog signaling maintains a tumor stem cell compartment in multiple myeloma. Proc Natl Acad Sci U S A 2007;104: 4048–53.
24. Ueno T, Toi M, Saji H, Muta M, Bando H, Kuroi K, et al. Significance of macrophage chemoattractant protein-1 in macrophage recruitment, angiogenesis, and survival in human breast cancer. Clin Cancer Res 2000;6:3282–9.
25. Kellermann MG, Sobral LM, da Silva SD, Zecchin KG, Graner E, Lopes MA, et al. Mutual paracrine effects of oral squamous cell carcinoma cells and normal oral fibroblasts: induction of fibroblast to myofibroblast transdifferentiation and modulation of tumor cell proliferation. Oral Oncol 2008;44:509–17.
26. Kojima Y, Acar A, Eaton EN, Mellody KT, Scheel C, Ben-Porath I, et al. Autocrine TGF-beta and stromal cell-derived factor-1 (SDF-1) signaling drives the evolution of tumor-promoting mammary stromal myofibroblasts. Proc Natl Acad Sci U S A 2010;107: 20009–14.
27. Qian DZ, Rademacher BL, Pittsenbarger J, Huang CY, Myrthue A, Higano CS, et al. CCL2 is induced by chemotherapy and protects prostate cancer cells from docetaxel-induced cytotoxicity. Prostate 2010;70:433–42.
28. Yu H, Kortylewski M, Pardoll D. Crosstalk between cancer and immune cells: role of STAT3 in the tumour microenvironment. Nat Rev Immunol 2007;7:41–51.
29. Soria G, Ben-Baruch A. The inflammatory chemokines CCL2 and CCL5 in breast cancer. Cancer Lett 2008;267:271–85.
30. Saji H, Koike M, Yamori T, Saji S, Seiki M, Matsushima K, et al. Significant correlation of monocyte chemoattractant protein-1 expression with neovascularization and progression of breast carcinoma. Cancer 2001;92:1085–91.
31. Lu X, Kang Y. Chemokine (C-C motif) ligand 2 engages CCR2+ stromal cells of monocytic origin to promote breast cancer metastasis to lung and bone. J Biol Chem 2009;284:29087–96.
32. Qian BZ, Li J, Zhang H, Kitamura T, Zhang J, Campion LR, et al. CCL2 recruits inflammatory monocytes to facilitate breast-tumour metastasis. Nature 2011;475:222–5.
33. de Vasconcellos JF, Laranjeira AB, Zanchin NI, Otubo R, Vaz TH, Cardoso AA, et al. Increased CCL2 and IL-8 in the bone marrow microenvironment in acute lymphoblastic leukemia. Pediatr Blood Cancer 2011;56:568–77.
34. Molloy AP, Martin FT, Dwyer RM, Griffin TP, Murphy M, Barry FP, et al. Mesenchymal stem cell secretion of chemokines during differentiation into osteoblasts, and their potential role in mediating interactions with breast cancer cells. Int J Cancer 2009;124: 326–32.
35. Ranganathan P, Weaver KL, Capobianco AJ. Notch signalling in solid tumours: a little bit of everything but not all the time. Nat Rev Cancer 2011;11:338–51.
36. Takebe N, Harris PJ, Warren RQ, Ivy SP. Targeting cancer stem cells by inhibiting Wnt, Notch, and Hedgehog pathways. Nat Rev Clin Oncol 2011;8:97–106.
37. Yashiro-Ohtani Y, He Y, Ohtani T, Jones ME, Shestova O, Xu L, et al. Pre-TCR signaling inactivates Notch1 transcription by antagonizing E2A. Genes Dev 2009;23:1665–76.
38. Meng W, Swenson LL, Fitzgibbon MJ, Hayakawa K, Ter Haar E, Behrens AE, et al. Structure of mitogen-activated protein kinase-activated protein (MAPKAP) kinase 2 suggests a bifunctional switch that couples kinase activation with nuclear export. J Biol Chem 2002;277:37401–5.
39. Page JL, Wang X, Sordillo LM, Johnson SE. MEKK1 signaling through p38 leads to transcriptional inactivation of E47 and repression of skeletal myogenesis. J Biol Chem 2004;279:30966–72.